Computer Assisted Mechanics and Engineering Sciences, **18**: 205–216, 2011.

Hybrid Monte Carlo method in the reliability analysis of structures

Joanna Kaliszuk
University of Zielona Góra
Prof. Z. Szafrana 1, 65-516 Zielona Góra, Poland
e-mail: j.kaliszuk@ib.uz.zgora.pl

The paper develops the idea of [8], i.e. the application of Artificial Neural Networks (ANNs) in probabilistic reliability analysis of structures achieved by means of Monte Carlo (MC) simulation. In this method a feed – forward neural network is used for generating samples in the MC simulation. The patterns for network training and testing are computed by a Finite Element Method (FEM) program. A high numerical efficiency of this Hybrid Monte Carlo Method (HMC) is illustrated by two examples of the reliability analysis that refer to a steel girder [4] and a cylindrical steel shell [2].

Keywords: reliability, Artificial Neural Networks (ANNs), Finite Element Method (FEM), Hybrid Monte Carlo Method (HMC), steel girder, cylindrical steel shell.

1. Introduction

The fully probabilistic reliability analysis of structures belongs to a group of very complicated problems for which obtaining an analytical solution is very difficult and frequently impossible. This explains why probabilistic analysis of structures needs numerous simulation methods, e.g. the Monte Carlo method [6]. In reliability analysis of structures by means of MC simulation the samples are usually computed by the FEM programs. A great number of samples is needed in the MC simulation, so the application of FEM program is numerically inefficient for large scale problems, because of high computational time. The most efficient, in terms of computation, is the so called hybrid Monte Carlo method, the idea of which was suggested by Papadrakakis et al. in [8]. This method applies simple, back – propagation neural networks (BPNNs) for generating trials in MC simulation. The BPNN is trained and tested on patterns generated by FEM program. A crucial question in the presented hybrid approach is a number of patterns needed for the network training and testing. This depends on the complexity of a structure analyzed and the number of random basic variables representing physical quantities of this structure. Two examples of HMC method application in reliability analysis is presented in this paper. The discussed reliability analyses concern a steel girder [4] and a cylindrical steel shell [2]. Other examples, corresponding to reliability of steel frames with random imperfections were analyzed in [1].

2. Reliability analysis by means of MC simulation method

It is assumed that reliability analysis refers to stationary type structural problems and the time factor is ignored. The adpted measure of structure reliability is the probability of reliability q, which is related to the probability of failure p_f, according to the following formula:

$$q = 1 - p_f \equiv 1 - \text{Prob}\left\{G(\mathbf{X}) \leq 0\right\}. \tag{1}$$

The probability of failure p_f is defined as a function of basic random variables:

$$p_f = \text{Prob}\left\{G(\mathbf{X}) \leq 0\right\} = \text{Prob}\left\{R\left(\mathbf{X}^R\right) - S\left(\mathbf{X}^S\right) \leq 0\right\} = \int\limits_{G(\mathbf{X})\leq 0} f\left(\mathbf{X}\right) d\mathbf{X}, \tag{2}$$

where: $G(\mathbf{X}) = G\left(\underline{R},\ \underline{S}\right) = \underline{R} - \underline{S}$ – the performance function; $\mathbf{X} = \left[\mathbf{X}^R, \mathbf{X}^S\right]$ – the vector of basic random variables, $\underline{R} = R\left(\mathbf{X}^R\right)$ – the random resistance, $\underline{S} = S\left(\mathbf{X}^S\right)$ – the actions (loads) applied to a structure, $f\left(\mathbf{X}\right)$ – the probability density function (PDF) of failure.

The MC simulation is applied in order to quantify the integral in (2). The approximate value of p_f is estimated by the binary MC indicator $I(\mathbf{X}_i)$ according to the formula:

$$\overline{p_f} = \frac{1}{NMC}\sum_{i=1}^{NMC} I\left(\mathbf{X}_i\right), \qquad I\left(\mathbf{X}_i\right) = \left(1 \quad \text{for} \quad G\left(\mathbf{X}_i\right) \leq 0 \quad \text{or} \quad 0 \quad \text{for} \quad G\left(\mathbf{X}_i\right) > 0\right), \tag{3}$$

where $\mathbf{X}_i = \left[\mathbf{X}_i^R, \mathbf{X}_i^S\right]$ – the vector of random variables of the performance function, $G\left(\mathbf{X}_i\right) = R\left(\mathbf{X}_i^R\right) - S\left(\mathbf{X}_i^S\right)$ – the value of performance function for the i-th sample, NMC – number of MC trials.

Formula (3) corresponds to the simplest MC method, called Crude or Classical MC (CMC) approach. The simulation result is reliable only with the use of a great number of MC samples. In case of reliability analysis of RC2 reliability class structure, according to [13], MC simulation needs greater than 10^8 samples ($NCM \geq 10^8$). That is why the neural networks are explored to a fast calculation of MC samples resistance.

3. Computation of training patterns

In the presented HMC method, the load capacity (resistance) of the structure corresponding to i-th randomly selected sample $\mathbf{X}_i$ is computed by means of ANN mapping:

$$\mathbf{X}_{N\times 1} = \{x_1,\ ...,\ x_n\} \quad \xrightarrow{ANN} \quad y = \lambda_{ult}, \tag{4}$$

where x_i – random variable corresponding to geometric values or material characteristics of the analyzed structure, λ_{ult} – ultimate load parameter.

Training and testing patterns of ANN are computed by means of FEM (COSMOS/M) program. In this case, the single load parameter is considered, $\mathbf{P} = \lambda_{ult}\mathbf{P}^*$, where $\mathbf{P}^*$ – the reference load vector. The ultimate load parameter λ_{ult} corresponds to the global buckling of the analyzed structure.

4. Examples of the reliabilty analysis by means of HMC method

4.1. Analysis of a steel girder

4.1.1. Data for a steel girder

The analyzed girder and its I-cross-section dimensions are shown in Fig. 1. The girder has only support stiffeners and the 4^{th} class cross-section conditions are fulfilled according to the classification of the Eurocode 3 [14]. The girder is assumed to be made of steel with the yield point $f_y = 235$ MPa and the stiffness modulus $E = 205$ GPa. The girder is subjected to the action of uniform load $S = P$ and the resistance of the structure corresponds to the ultimate load $R = \lambda_{ult}P^*$, where $P^* = 200$ kN/m is the reference load.

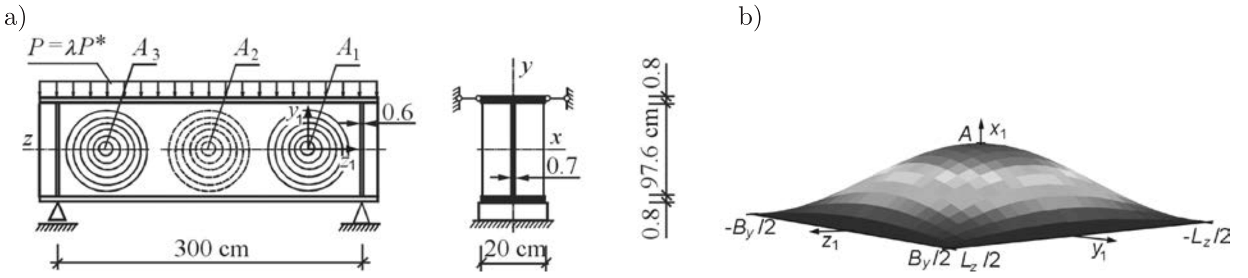

Fig. 1. a) The scheme of Steel girder, b) the model of web plate imperfections.

The initial imperfections of the web plate are considered. This imperfections are modeled as three smooth surfaces of the form taken from [5]:

$$w_k(y_1,\, z_1) = A_k \cos\left(\pi y_1/B_y\right) \cos\left(\pi z_1/L_z\right), \tag{5}$$

where A_k – the amplitudes of imperfections; $B_y = L_z = 97.6$ cm – the ranges of imperfections.

It was assumed that the imperfections can randomly appear in three equidistant areas $B_y \times L_z$. The amplitudes A_k are random variables of the normal probability density function with parameters: $\mu_{Ak} = 0$ mm and $\sigma_{Ak} = A_{ult}/2 = 0.35$ cm, where $A_{ult} = 0.7$ cm is the admissible value according to the Polish standard PN-B-6200 [12].

4.1.2. Generation of training and testing patterns

Training and testing patterns were computed by the FEM program COSMOS/M [10]. A nonlinear module of the program was explored assuming an elastic-plastic material with Huber-von Mises yield surface and isotropic linear strain hardening with $E_p = 0.0001E$.

The training patterns were computed for the input data placed regularly in the 3D-cube of coordinates $A_k \in [-3\sigma_{Ak},\ 3\sigma_{Ak}]$. Assuming 5 points at the A_k axes the number of training patterns equals $L = 3^5 = 125$ cf. Pabisek et al. [6]. The set of $T = 100$ testing patterns was randomly selected as 100 points in the 3D-cube of variables A_k, assuming normal PDF, with the same parameters as for the training patterns.

In Fig. 2 the equilibrium path $\lambda(v_0) \in [1.180, 1.393]$ computed for the input data $A_1 = -0.525$ cm, $A_2 = 1.05$ cm, $A_3 = 1.05$ cm is shown.

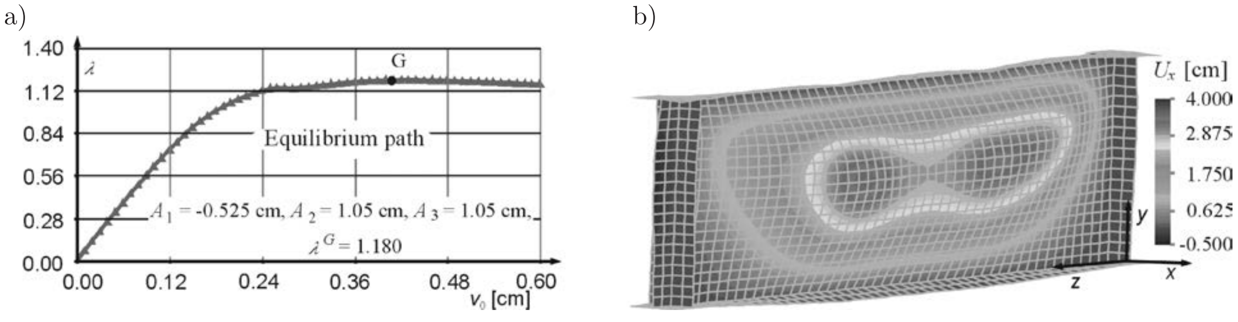

Fig. 2. a) The equilibrium path, b) the displacements of girder at load factor $\lambda^G = 1.180$.

The ultimate state of the girder corresponds to the load parameter $\lambda^G = \lambda^G_{\min} = 1.180$. This state is related to the overall instability of the girder caused by the buckling of the upper flange and the web plate. In case of the perfect girder, i.e. for $A_1 = A_2 = A_3 = 0$ the ultimate load parameter is $\lambda^G_{perf} = 1.248$ and for the initial imperfections $A_1 = -1.05$ cm, $A_2 = 0.525$ cm, $A_3 = -1.05$ cm the ultimate load corresponds to $\lambda^G = \lambda^G_{\max} = 1.393$. The average CPU time to compute one pattern was about 300 sec.

4.1.3. Design of neural network

The back-propagation neural network was designed by means of Neural Network Toolbox [10] which was implemented in the frame of MATLAB packages. The following input vector and output scalar were used:

$$\mathbf{X}^R = \{A_1,\ A_2,\ A_3\}\,, \qquad y = \lambda_{ult} \tag{6}$$

to formulate the set of training and testing patterns:

$$\mathcal{L} = \{(\mathbf{X}^R, t)_p \backslash p = 1, ..., L\}, \tag*{(7)$_1$}$$

$$\mathcal{T} = \{(\mathbf{X}^R, t)_p \backslash p = 1, ..., \mathrm{T}\}, \tag*{(7)$_2$}$$

where t – the target output computed by FEM; $L = 125$ – the number of training patterns related to regular points in 3D input cube; $T = 100$ – the number of testing patterns corresponding to randomly selected points in 3D cube.

The BPNN network of structure 3-H-1 with sigmoidal hidden neurons and linear output was designed using the cross-validation procedure [9] supported on the sets (7). The Levenberg-Marquardt learning method was used. The number of hidden neurons $H_{opt} = 8$ was determined. The accuracy of the designed network can be evaluated by the relative errors

$$\mathrm{avr}\, epV = \frac{1}{V}\sum_{p=1}^{V} ep, \qquad \max\, epV = \max_{p} ep, \tag{8}$$

where $ep = (1 - y_p/t_p){\cdot}100\%$ – the relative error for the p-th pattern; $V = L,\ T$ – errors for the training and testing.

Another estimation is given by statistical parameters, i.e. the standard error $St\varepsilon V$ and the correlation parameter rV, cf. Waszczyszyn and Ziemiański [9].

$$St\varepsilon V = RMSE = \frac{1}{\sqrt{V}}\sqrt{\sum_{p=1}^{V}\Big((t_p - y_p)^2\Big)}\,, \tag{9}$$

where $V = L,\ T$ – the number of patterns for the network training and testing, respectively, t_p, y_p – the output values for known and neurally computed output for the p-th patern.

In case of the trained network BPNN: 3-8-1 the errors are: $\mathrm{avr}\, epL \approx \mathrm{avr}\, epT = 0.77\%$, $\max epL \approx \max epT = 3.90\%$, $St\varepsilon L \approx St\varepsilon T = 0.0136$, $rL = 0.959$, $rT = 0.790$. In Fig. 3 the relations of the FEM target values t_p and neurally predicted outputs y_p are shown.

4.1.4. Reliability analysis of considered girder

The designed network BPNN: 3-8-1 was used for the simulation of MC trials. First of all, it was checked that for computing 10^8 MC trials the network consumed 416 s of CPU time. This time is comparable with 300 s needed for the computation of one pattern by the FEM system COSMOS/M.

Next, the network was used for the computation of discrete points at the reliability curves $\overline{q}(P)$, where $\overline{q}$ is the estimated value of the probability of reliability, according to formula (1) and $P = S$ is the load applied to the girder.

In the definition of the reliability curve there are two cases corresponding to the assumption of the action variable: 1) Case 1: load P is the random value and the normal PDF has parameters $\overline{P}_j = \mu_{Pj}$, $\overline{\sigma}_{Pj} = 0.1\overline{P}_j$, 2) Case 2: P_j is the deterministic real value. In Fig. 4 there are two curves corresponding to both cases. It is worth mentioning that in Case 1 the reliability curve $\overline{q}\left(\overline{P}_j\right)$ is smooth, without discontinuity type parts which occur in Case 2 of the curve $\overline{q}\,(P_j)$.

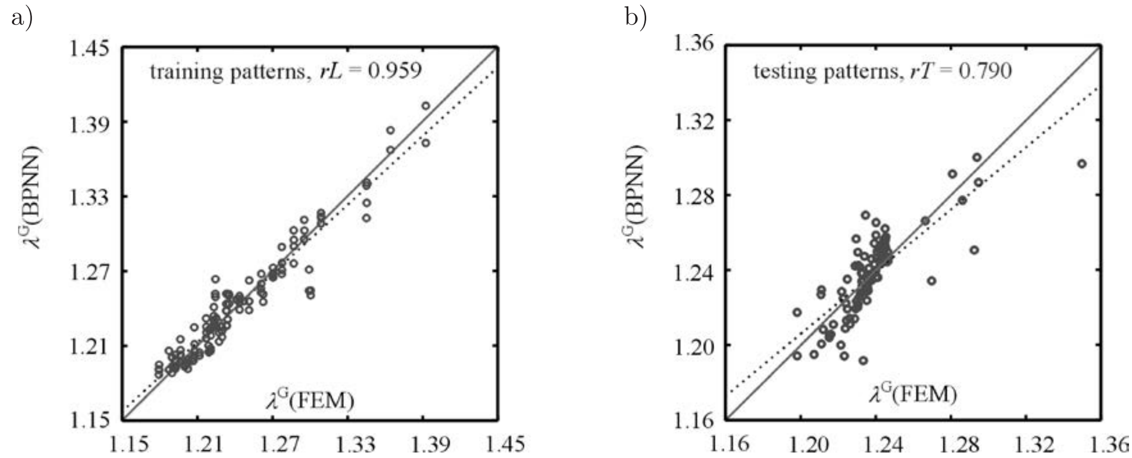

Fig. 3. Correlation of patterns computed by FEM and BPNN.

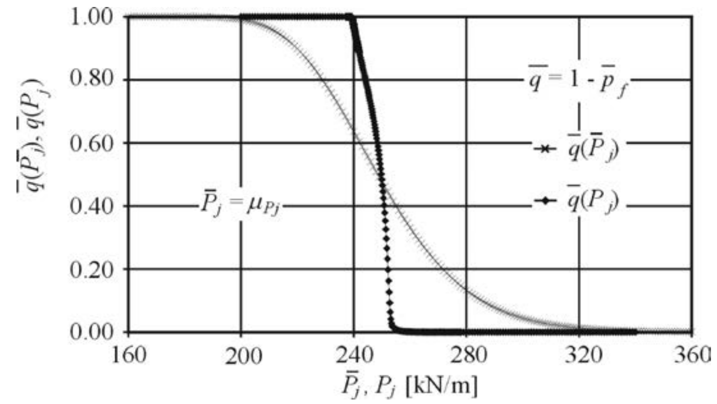

Fig. 4. Reliability curves for random loads $\overline{P}_j$ and deterministic loads P_j.

4.1.5. Analysis of CPU times

Table 1 lists CPU times corresponding to computation of the reliability curve $\overline{q}\left(\overline{P}_i\right)$ for two numerical versions of CMC simulations: 1) the hybrid version FEM/BPNN, 2) FEM is hypothetically used for the computer simulation of the same number of MC trials as in the hybrid version.

Table 1. The comparison of CPU times for two numerical versions of CMC (Classical Monte Carlo method).

Simulation of CMC trials by BPNN: 3-8-1		Simulations of CMC trials by FEM system COSMOS/M	
Operations	CPU time [s]	Operations	CPU time [s]
Preparation of 225 patterns by FEM, 225·300 =	67500	Computation of one pattern	300
Training and testing of BPNN, = about 20 hrs	72000	Hypothetical computations of 10^8 trials	$300{\cdot}10^8$
Simulation of 10^8 CMC trials	416	Total CPU time	$3.0{\cdot}10^{10}$
Total CPU time	$1.4{\cdot}10^5$		

Application of the hybrid FEM/BPNN method needs $1.4 \cdot 10^5$ s $\approx$ 39 hrs = 1.62 days. The hypothetical time of computing 10^8 CMC trials by the FEM system COSMOS/M equals about $3.0 \cdot 10^{10}$ s $\approx 3.47 \cdot 10^5$ days. This gives the computation 200 000 times longer than for the CPU time needed for the hybrid method.

4.1.6. Conclusions

- The reliability curves for a steel girder of I cross-section can be very efficiently computed by means of the hybrid Monte Carlo approach in which 225 patterns are computed by the FEM system COSMOS/M. Then these patterns are used to design the neural network BPNN:3-8-1. The trained network was used for simulation of 10^8 trials of the Classical Monte Carlo method.
- The analysis of CPU times gives a hypothetical evaluation of numerical efficiency of the considered Hybrid Monte Carlo approach. This method applied for three random amplitudes of the girder web plate needs about $2.0 \cdot 10^5$ times lower CPU time than that time needed for the trial simulations by the COSMOS/M system.

4.2. Analysis of steel cylindrical shells

The analysis refers to three, laterally loaded cylindrical shells which were tested in laboratory. The numerical FEM model of shell was formulated on the basis of laboratory tests results. Detailed description of this laboratory tests and modeling process is in [3].

4.2.1. Laboratory tests on cylindrical shells

A scheme of the tested shell is shown in Fig. 5. In the scheme the important control parameter is shown corresponding to the stiffness of equivalent perfect rigid-plastic rods modeling the horizontal shift ability of the screws blocking the vertical displacements of the supporting beams.

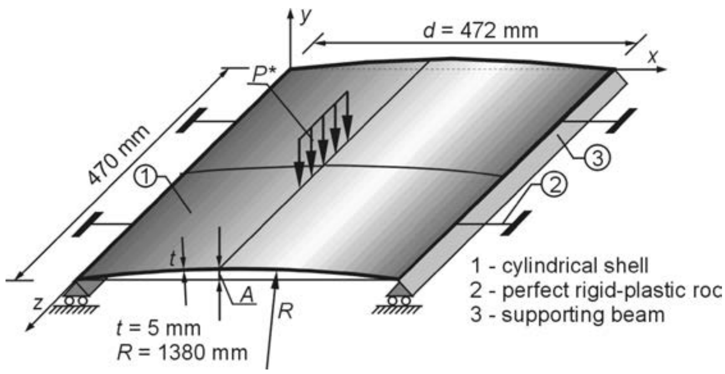

Fig. 5. Scheme of cylindrical shell.

Three shells were tested by means of the stand shown in Fig. 6.

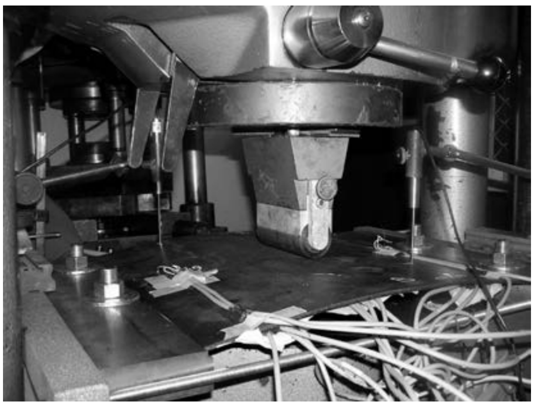

Fig. 6. Test stand.

The tested shells were made of a cold rolled sheet of 5 mm thickness. The shells were subjected to stress relief annealing to remove residual stresses formed in the steel sheet in the process of rolling and bending. Material parameters for elasto-plastic bilinear shell material model were identified in tension tests made on annealed steel sheet stripes. Mechanical parameter mean values were adopted as: E = 205 GPa, R_e = 274 MPa, ν = 0.3. The rectangular projection of the shell midsurfaces had dimensions $L \times B = 472 \times 470$ mm and curvature radius $R = 1380$ mm. The shell was placed between steel supporting beams of thickness $t_{BP} = 40$ mm, screwed to the lower crosshead plate of the test stand.

The deformation process was carried out by a slow motion of the pressing shaft fastened to the upper crosshead of the testing machine (see Fig. 6). The deformation process was continued until the load carrying capacity was reached. The form of incrementing plastic deformations registered in the tests corresponded with the three linear plastic hinges with the dominating central hinge.

4.2.2. Updating of a FEM model and computation of patterns

A numerical FE model of the shell was prepared in COSMOS/M program. In numerical modeling of the shell the geometrical and material data obtained in particular tests were used.

The shell, truss (rod) and beam finite elements were applied in the modeling process. The shell material was modeled as elasto-plastic one with the Huber – Mises – Hencky plasticity condition and isotropic hardening. A finite element mesh for the whole model is shown in Fig. 7. Types of finite elements used in the numerical model and material properties of this elements are placed in Table 2.

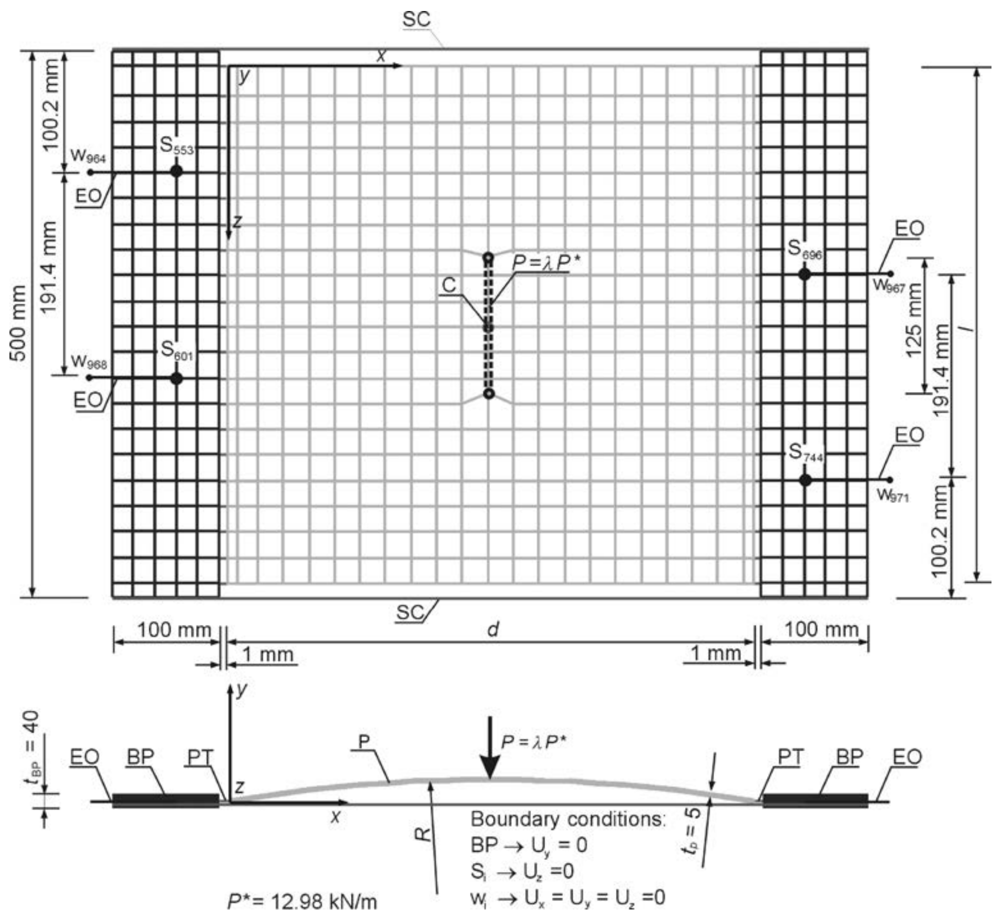

Fig. 7. FEM model.

Table 2. Finite elements in adjusted numerical model.

Part of model	Type of FE	Material model	R_e [MPa]	E [GPa]	E_T [MPa]	ν
P	SHELL4T	bilinear	274	205	20.5	0.3
BP	SHELL4T	bilinear	235	205	20.5	0.3
PT	BEAM3D	linear	235	205	–	0.3
SC	TRUSS3D	linear	640	205	–	–
EO	TRUSS3D	linear	235	5000	0.05	–

In the Table 2: bilinear = elasto-plastic HMH material with isotropic strain hardening, linear = perfectly elastic material, R_e – yield stress, E – elastic modulus, E_T – hardening modulus, ν – Poisson's coefficient.

The numerical analysis was carried out with the use of nonlinear module of COSMOS/M program. Figs. 8 and 9 present the exemplary results of FE simulation. A comparison of displacement equilibrium paths obtained from the laboratory test and its equilibrium paths FE simulation are shown in Fig. 8. A coincidence of the comparison resulting solutions is very good. Fig. 9 shows equivalent stress distribution on the upper surface of the shell for the maximum pressure force value.

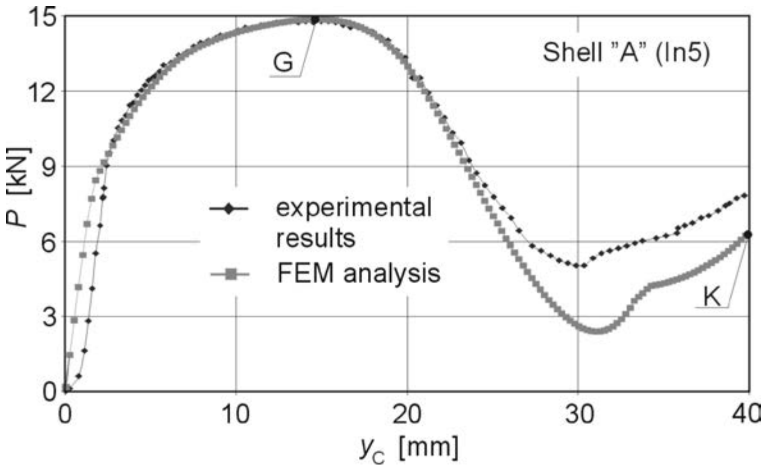

Fig. 8. Shell displacement equilibrium paths.

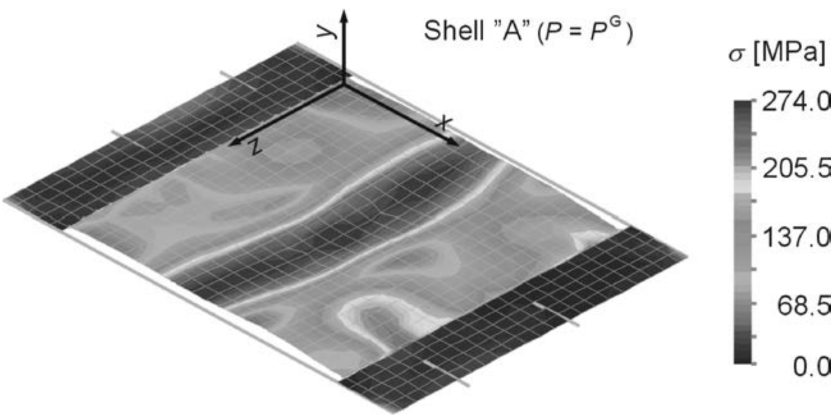

Fig. 9. Equivalent stresses in the upper shell surface.

The adjusted numerical model was used in the sensitivity analysis which was performed in order to select a group of parameters significantly affecting the random resistance of the shells under analysis. The following three control parameters were selected in the FE model: A – the approximated deflection of the cylindrical shell midsurface, R_e – the yield stress, A_T – the cross-section of the equivalent rods preventing lateral displacement of supports (elements specified as EO in Fig. 7).

Those selected parameters were included to the shell reliability analysis as the basic random variables related to the random resistance of the considered shell. Two cases of a vector of random variables $\mathbf{X}^R$ were considered: 1) $\mathbf{X}^R = \{A^*, R_e, A_T\}$, where A^* – the rise of the segment of the cylinder approximating the real geometry of the shell, 2) $\mathbf{X}^R = \{A_1, A_3, R_e, A_T\}$, where A_1, A_3 – amplitudes of trigonometric functions approximating a real surface of the shell. It was assumed that the yield stress R_e and deflection parameters A^*, A_1, A_3 have the normal PDF whereas the cross-section A_T has the lognormal PDF. The parameters of probability distributions of admitted random variables are collected in Table 3.

Table 3. Distribution parameters of random variables.

Random variable		R_e [MPa]	A_T [mm^2]	A^* [mm]	A_1 [mm]	A_3 [mm]
Type of PDF		N	LN	N	N	N
Parameters of PDF	μ	307.1	4.095	22.20	22.69	0.760
	σ	30.71	0.292	2.22	2.269	0.152

In the Table 3: N – normal distribution, LN – lognormal distribution.

For each of both mentioned cases three sets of training patterns were calculated with the use of the prepared FE model. Those pattern sets have different number L_{ij} of elements: $L_{11} = 3^3 = 27$, $L_{12} = 5^3 = 125$, $L_{13} = 7^3 = 343$ for the case 1) and $L_{21} = 3^4 = 81$, $L_{22} = 4^4 = 256$, $L_{23} = 5^4 = 625$ for the case 2), where i – the case number of a vector of random variables, j – the number of training pattern set. The elements of the sets cover evenly the space of random variables which was limited by extreme values $\mu \pm 3\sigma$ of each random variable respectively. The sets of testing patterns were randomly selected from this limited space of random variables. The $T_k = 100$ testing patterns were calculated for each of the cases considered.

4.2.3. Design, training and testing of BPNNs

The Back-Propagation Neural Networks (BPNNs) were assumed with one hidden layer of the structure N-H-1. Sigmoid binary activation functions were used in the hidden layer and identity function in the output neuron. Two types of BPNNs were prepared corresponding to two cases of vectors of basic random variables $\mathbf{X}^R$, described above in point 4.2.2. Those BPNNs perform the mapping as follows:

$$\mathbf{X}^R = \{A^*, R_e, A_T\} \xrightarrow{\text{BPNN}} y = \lambda_{ult} \qquad \text{for} \quad \text{Case 1,} \tag{10$_1$}$$

$$\mathbf{X}^R = \{A_1, A_3, R_e, A_T\} \xrightarrow{\text{BPNN}} y = \lambda_{ult} \qquad \text{for} \quad \text{Case 2.} \tag{10$_2$}$$

Three families of networks were trained for each of the both considered cases, each of which was trained using a different set of training patterns with the number L_{ij} of elements. The method of generating those pattern sets are presented in point 4.2.2. Six best networks, one from each of network family, with the least error values of neural approximation was selected. The Table 4 lists the selected BPNNs with their training and testing errors which were calculated as standard errors $St\varepsilon V$ and average relative errors avr epV, $V = L, T$ – errors for the training and testing.

Table 4. Training and testing errors of selected BPNNs.

Type	BPNN_{ij}	L_{ij}	N-H-1	$St\varepsilon^{*}10^{2}$		avr ep [%]	
				L	T	L	T
1	BPNN 11	27	3-3-1	3.08	2.44	0.33	0.18
	BPNN 12	125	3-11-1	0.50	0.67	0.05	0.06
	BPNN 13	343	3-14-1	0.37	0.62	0.04	0.06
2	BPNN 21	81	4-5-1	2.89	1.58	0.27	0.16
	BPNN 22	256	4-13-1	0.60	0.90	0.06	0.09
	BPNN 23	625	4-12-1	0.69	0.66	0.06	0.06

In the Table 4: i – the number of network type, j – number of network family.

4.2.4. Reliability analysis of a steel cylindrical shell

The selected trained BPNNs were used for efficient calculation of random trials in Crude Monte Carlo (CMC) simulations, which were carried out to compute the reliability curves. Two cases of CMC simulation were performed. The cases differed in the formulation of the load: Case I – the load P is a determined value and a reliability curve $\overline{q}(P)$, computed for a sequence of fixed loads P_i, and assuming load step ΔP, Case II – load P is a random variable with the average $\overline{P}$ and coefficient of variation $V = 0.1$. In this case a reliability curve $\overline{q}\left(\overline{P}\right)$ is computed for a sequence of determined mean values of random load $\overline{P}_i$ with load step $\Delta\overline{P}_i$.

Twelve structural reliability curves were computed which referred to each particular Case of CMC simulation, cases of basic random variables $\mathbf{X}^R$ vectors and family of BPNNs. In order to have statistically representative sets, 10^8 trials were generated in each simulation.

In Fig. 10 all the curves obtained in the reliability analysis are presented. Each of them is related to Case ijk of reliability analysis, where indexes i,j,k refer to case of CMC simulation (i = I, II), case of the random variables vector (j = 1, 2) and family of BPNNs (k = 1, 2, 3), respectively. In Case I and Case II of CMC simulation, six computed curves overlap, this means that the results of CMC simulations with the use of: BPNNs: BPNN: 3-14-1 trained by means of $L = 343$ patterns, BPNN: 3-3-1, trained by means of $L = 27$ patterns, BPNN: 4-12-1 trained by $L = 625$ patterns and BPNN:

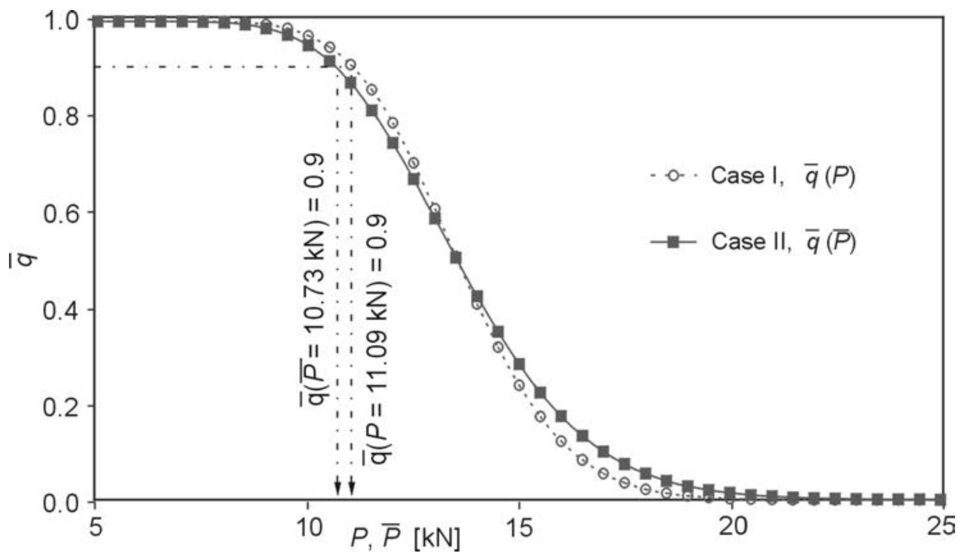

Fig. 10. Structural reliability curves: six curves related to Case I, and six curves related to Case II.

4-5-1 trained by 81 patterns, respectively, are almost the same. That is why in Fig. 10 it seems, that there are only two reliability curves, related to the simulations in Case I and Case II, respectively. It was shown in this figure that reliability analyses according to the considered two load cases give results close to each other. For instance, for desirable probability of reliability $\overline{q}\left(\overline{P}\right) = \overline{q}(P) = 0.9$ the corresponding mean value of load is $\overline{P} \approx 10.73$ kN and the fixed load value is $P \approx 11.09$ kN.

4.2.5. Analysis of CPU times

CPU times analysis refer to CMC simulations with the use of 10^8 trials. CMC simulation with the use of BPNN: 3-3-1 was ended after $0.7 \cdot 10^4$ s and was the fastest of the simulations with other BPNNs. The simulation with BPNN: 4-13-1 was the slowest and was evaluated for $1.5 \cdot 10^4$ s. When the time of BPNNs formulation and generating of training and testing patterns are taken to account the HMC reliability analysis with BPNN: 4-13-1 needs $1.1 \cdot 10^5$ s.

In case of computing by the FE program COSOS/M the time of generating one pattern was about 280 s. Thus, assuming hypothetically that 10^8 trials are generated by COSMOS/M, then the CPU execution time would be ca. $2.8 \cdot 10^{10}$ s, that is ca. $2.5 \cdot 10^5$ times higher than the neural simulation time. The comparison of the CPU time needed to reliability analysis with the use of HMCM method with the hypothetical time needed to analysis by means of the MC simulation with FE computation of trials, is presented in the Table 5.

Table 5. CPU times analysis.

<table>
<tr><td colspan="2">Simulation of CMC trials by BPNN: 4-13-1</td><td colspan="2">Simulations of CMC trials by FEM system COSMOS/M</td></tr>
<tr><td>Operations</td><td>CPU time [s]</td><td>Operations</td><td>CPU time [s]</td></tr>
<tr><td>Preparation of 725 patterns by FEM, 725·280 =20300</td><td>20300</td><td>Computation of one pattern</td><td>280</td></tr>
<tr><td>Training and testing of BPNN, = about 20 hrs</td><td>72000</td><td>Hypothetical computations of 10^8 trials</td><td>$280 \cdot 10^8$</td></tr>
<tr><td>Simulation of 10^8 CMC trials</td><td>15000</td><td rowspan="2">Total CPU time</td><td rowspan="2">$2.8 \cdot 10^{10}$</td></tr>
<tr><td>Total CPU time</td><td>$1.1 \cdot 10^5$</td></tr>
</table>

4.2.6. Conclusions

The presented reliability analysis of the steel shell confirms very high efficiency of hybrid MC method.

The comparison of reliability curves obtained in HMC simulations shows the possibility of limitation of patterns number, needed for neural networks training.

5. Final conclusions

Application of ANN for generating trials in MC simulations significantly decreases the computation time in comparison with the hypothetical computation time while generating trials only by means of FEM.

The total computation time of the hybrid MC method strongly depends on the number of the patterns generated by FEM for the training and testing of ANN. That is why, conducting the sensitivity analysis of construction for selecting the basic variables set $\mathbf{X}^R$ with the smallest number of elements, is very important.

HMC method gives a possibility to make the reliability analysis of many real structures tested.

References

[1] J. Kaliszuk. *Reliability analysis of construction and construction elements using artificial neural networks* (in Polish). Ph.D. Thesis, University of Zielona Góra, 2005.

[2] J. Kaliszuk. Updating of FEM Models for laboratory tests on cylindrical panels and their reliability analysis by the hybrid FEM/ANN Monte Carlo method. In: A. Borkowski, T. Lewiński, [Eds.],*19th International Conference on Computer Methods in Mechanics. Short Papers*, 235-236, Publishing House of the Warswa University of Technology, Warszawa, 2011.

[3] J. Kaliszuk, J. Marcinowski, Z. Waszczyszyn. Experimental Investigation and Numerical Modelling of Large Displacements of Elasto-plastic Cylindrical Shell. In: W. Pietraszkiewicz, C. Szymczak, [Eds.], *SSTA 8: Shell Structures: Theory and Applications, Proceedings of the 8th SSTA Conference*, 477–480. Taylor & Francis, London, 2005.

[4] J. Kaliszuk, Z. Waszczyszyn. Reliability analysis of a steel girder by the hybrid FEM/BPNN Monte Carlo method. In: M.A. Giżejowski, A. Kozłowski et al., [Eds.], *Progress in Steel, Composite and Aluminium Structures: Proc. XI^{th} Intern. Conf. on Metal Structures*, 346–347. Taylor& Francis Group, London, 2006.

[5] M. Królak. *Postcritical behaviour and load carrying capacity of thin-walled girders* (in Polish). PWN, Warszawa, 1990.

[6] P. Marek, M. Guštar, Th. Anagnos. *Probabilistic Assessment of Structures using Monte Carlo Simulation.* TeReCo, 2001.

[7] E. Pabisek, J. Kaliszuk, Z. Waszczyszyn. Neural and finite element analysis of a plane steel *frame* reliability by the Classical Monte Carlo method. In: L. Rutkowski, J. Siekmann, R. Tadeusiewicz, L.A. Zadeh, [Eds.], *Artificial Intelligence and Soft Computing, Proc. 7^{th} Intern. Conf., Zakopane, 2004*, 1081–1086. Springer, Heidelberg, 2004.

[8] M. Papadrakakis, V. Papadopoulos, N.D. Lagaros. Structural reliability analysis of elastic-plastic structures using neural networks and Monte Carlo simulation. *Computer Methods in Applied Mechanics and Engineering*, **136**: 145–163, 1996.

[9] Z. Waszczyszyn, L. Ziemiański. Neural networks in the identification analysis of structural mechanics problems. In: Z. Mróz, G.E. Stavroulakis, [Eds.], *Parameter identification of materials and structures. CISM Courses and Lectures*, **469**: 265–340. Springer, Wien-New York, 2005.

[10] *COSMOS/M, Finite element analysis system. Version 2.5.* Structural Research and Analysis Corp., California: Los Angeles, 1999.

[11] *Neural Network Toolbox for Use with MATLAB*, User's *Guide, Version 3.* The Math Works, Inc., Natick, MA, 1998.

[12] PN-B-06200. *Building steel structures. Requirements for production and control. Basic requirements.* PKN, Warszawa, 2002.

[13] PN-EN 1990. *Eurocode: Basis of structural design.* PKN, Warszawa, 2004.

[14] PN-EN 1993. *Eurocode 3: Design of steel structures.* PKN, Warszawa, 2006.